



Heriot-Watt University
Research Gateway

Wideband Bandpass Filters Based on Eighth-Mode Substrate Integrated Waveguide and Microstrip Resonators

Citation for published version:

Weng, X, Xu, K-D & Fan, H 2023, 'Wideband Bandpass Filters Based on Eighth-Mode Substrate Integrated Waveguide and Microstrip Resonators', *IEEE Transactions on Circuits and Systems II: Express Briefs*, vol. 70, no. 7, pp. 2375-2379. <https://doi.org/10.1109/TCSII.2023.3244791>

Digital Object Identifier (DOI):

[10.1109/TCSII.2023.3244791](https://doi.org/10.1109/TCSII.2023.3244791)

Link:

[Link to publication record in Heriot-Watt Research Portal](#)

Document Version:

Peer reviewed version

Published In:

IEEE Transactions on Circuits and Systems II: Express Briefs

Publisher Rights Statement:

© 2023 IEEE. Personal use of this material is permitted. Permission from IEEE must be obtained for all other uses, in any current or future media, including reprinting/republishing this material for advertising or promotional purposes, creating new collective works, for resale or redistribution to servers or lists, or reuse of any copyrighted component of this work in other works.

General rights

Copyright for the publications made accessible via Heriot-Watt Research Portal is retained by the author(s) and / or other copyright owners and it is a condition of accessing these publications that users recognise and abide by the legal requirements associated with these rights.

Take down policy

Heriot-Watt University has made every reasonable effort to ensure that the content in Heriot-Watt Research Portal complies with UK legislation. If you believe that the public display of this file breaches copyright please contact open.access@hw.ac.uk providing details, and we will remove access to the work immediately and investigate your claim.

Wideband Bandpass Filters Based on Eighth-Mode Substrate Integrated Waveguide and Microstrip Resonators

Xiaoyu Weng, *Student Member, IEEE*, Kai-Da Xu, *Senior Member, IEEE*, and Haijun Fan, *Member, IEEE*

Abstract—A class of wideband bandpass filters (BPFs) with two eighth-mode substrate integrated waveguides (EMSIW) and two microstrip resonators is presented in this brief. The quarter-wavelength microstrip resonator is connected to the hypotenuse side of EMSIW resonator, which is different from these filters with two EMSIW resonators sharing vias or iris windows. By introducing the quarter-wavelength microstrip resonators, the design flexibility can be improved with a compact size. Based on the proposed topology, a BPF centered at 4 GHz is designed and fabricated with fractional bandwidth (FBW) of 25%. The measured insertion loss within the passband is only 0.9 dB, while the return loss is better than 14.1 dB. To further improve the roll-off skirts and attain a better out-of-band rejection, a transmission zero (TZ) is generated with the mixed electric and magnetic coupling between two microstrip resonators. The measured FBW of the BPF with one TZ is 26.6%, whose center frequency is also at 4 GHz. The measured stopband rejection above the passband is better than 34 dB from 5.02 to 8.31 GHz. Good agreement between simulated and measured results validates the feasibility of the proposed BPFs.

Index Terms—Bandpass filters, filter synthesis, microstrip resonator, mixed coupling, substrate integrated waveguide.

I. INTRODUCTION

WITH the rapid development of the modern wireless communication system, the substrate integrated waveguide (SIW) has been of great interest in the filter design because of its advantages of low loss, high Q-factor and ease of integration. However, the size of conventional SIW resonators is relatively large. To miniaturize SIW filters, several techniques have been proposed without affecting the characteristics of SIW, such as folded ridged SIW [1-2], half-mode SIW (HMSIW) [3], quarter-mode SIW (QMSIW) [4] and eighth-mode SIW (EMSIW) [5]. Due to the symmetrical characteristic, the HMSIW, QMSIW and EMSIW cavity present a similar field distribution compared with the conventional SIW cavities.

To obtain better performance, several flexible designs of bandpass filters (BPFs) have been reported by combining these abovementioned techniques with each other [6]–[9], or with

coplanar waveguide (CPW) [10]–[13] and microstrip structures [14]–[21]. In [7], the QMSIW and EMSIW cavities are exploited to design two BPFs. Cavities are coupled through the co-shared iris window and the feedlines are located at the open sides. However, such configuration will occupy a large footprint. To achieve compact size, QMSIW cavities and EMSIW cavities could be arranged in different layers, which is utilized to design a multilayer low-temperature co-fired ceramic (LTCC) dual-passband filter in [8]. Besides, a second-order EMSIW BPF is proposed for the design of a low phase noise oscillator [9], where the hypotenuse side of two EMSIW resonators are close to each other with controllable coupling.

Moreover, CPW structures could be embedded into SIW structures, which will combine the advantages of two structures together. In [10], filters based on hybrid structure of SIW and CPW are proposed, which could facilitate the generation of transmission zeros (TZs) by introducing the mixed coupling. In [11], a quarter-wavelength CPW resonator and a half-wavelength CPW resonator are embedded into an HMSIW cavity to realize the BPF with extended-doublet topology. Besides, a fourth-order filter with cross coupling is achieved with the combination of two CPW resonators and a pair of magnetically coupled QMSIW cavities, as shown in [13]. Similarly, there is enough area for SIW structures to house microstrip resonators. For instance, a miniaturized BPF is proposed using QMSIW cavities and meandering microstrip resonators [16], where two quarter-wavelength microstrip resonators are embedded into two back-to-back QMSIW cavities.

The topology of EMSIW cavity is a good candidate for the design of compact BPFs. Because it is a right triangle with one metallic wall and two open sides, it will influence the design flexibility if the back-to-back coupled structure is utilized between two EMSIW resonators with co-sharing vias. Besides, it is difficult to incorporate the CPW structure and microstrip resonators into the EMSIW resonators due to the limited area. In this paper, two wideband BPFs are proposed based on EMSIW resonators and microstrip resonators. Different from previously reported filters with two EMSIW resonators sharing vias, the EMSIW resonators in the proposed filters are separated without co-sharing iris window, while two quarter-wavelength microstrip resonators are connected to the open sides of EMSIW resonators. The enough area between separated EMSIW resonator cavities makes it possible to

This work was supported in part by the NSAF Joint Fund under Grant U2130102, and in part by “Siyuan Scholar” Fellowship of XJTU. (Corresponding author: Kai-Da Xu)

Xiaoyu Weng and Kai-Da Xu are with the School of Information and Communications Engineering, Xi’an Jiaotong University, Xi’an 710049, China. (e-mail: kaidaxu@ieee.org)

Haijun Fan is with the Institute of Sensors Signals and Systems, Heriot-Watt University, Edinburgh EH14 4AS, U.K.

change the configuration of microstrip resonators. With the electric coupling provided by two microstrip resonators, a Chebyshev frequency response can be easily achieved. Further improvement on out-of-band rejection can be attained with a TZ above the passband, through introducing the mixed electric and magnetic coupling. Besides, the size of EMSIW cavity is taken into consideration during the extraction process, which reduces the difficulty of optimization after the initial dimensions are determined. For demonstration, two BPFs (i.e., BPF I and BPF II) are designed with center frequencies at 4 GHz.

II. BPF I USING EMSIW AND MICROSTRIP RESONATORS

Fig. 1(a) presents the structure of the proposed BPF I, which has rotational symmetry and consists of two 50-Ω feed lines, two EMSIW resonators and two microstrip resonators. The quarter-wavelength microstrip resonator is connected to the hypotenuse side of EMSIW resonator, while metallic vias and feed line are arranged at the other two sides of EMSIW resonator, respectively. As reported in [9] and [17], two EMSIW resonators placed with central symmetry can build up a bandpass filter, whose bandwidth is limited by the gap-coupling structure and the number of resonators. However, adding EMSIW resonators will occupy too much area. Therefore, two microstrip resonators are introduced to provide the signal path between the two EMSIW resonators. Because of the meander structure of microstrip line, the design flexibility can be improved with a compact size. Fig. 1(b) shows the coupling topology of BPF I, where the hollow circles, shaded circles and solid circles represent the source/load, EMSIW resonators and microstrip resonators, respectively. Due to the symmetry structure of BPF I, the coupling topology is symmetric as well.

Based on the layout of BPF I, a fourth-order Chebyshev BPF is synthesized with a return loss (RL) of 15 dB in passband [22]. The coupling matrix \mathbf{M} can be derived as follows:

$$\mathbf{M} = \begin{bmatrix} 0 & S & 1 & 2 & 3 & 4 & L \\ S & 0 & -0.915 & 0 & 0 & 0 & 0 \\ 1 & -0.915 & 0 & -0.802 & 0 & 0 & 0 \\ 2 & 0 & -0.802 & 0 & 0.643 & 0 & 0 \\ 3 & 0 & 0 & 0.643 & 0 & -0.802 & 0 \\ 4 & 0 & 0 & 0 & -0.802 & 0 & 0.915 \\ L & 0 & 0 & 0 & 0 & 0.915 & 0 \end{bmatrix}, \quad (1)$$

whose coupling topology is the same as that of the proposed filter shown in Fig. 1(b). To obtain the BPF with center frequency of 4 GHz and equal-ripple fractional bandwidth (FBW) of 25%, the corresponding external quality factor (q_e) and coupling coefficients (k_{12} , k_{23}) can be calculated from entries of \mathbf{M} [23]:

$$q_e = \frac{1}{m_{S1}^2 \cdot FBW} = 4.78 \quad (2a)$$

$$k_{12} = |m_{12} \cdot FBW| = 0.2 \quad (2b)$$

$$k_{23} = |m_{23} \cdot FBW| = 0.16 \quad (2c)$$

When BPF I is implemented on a substrate with a thickness of 1 mm and ϵ_r of 2.65, the external quality factor and coupling coefficients between adjacent resonators could be numerically extracted by electromagnetic simulation. To distinguish from the calculated q_e , k_{12} and k_{23} , the extracted results of external quality factor and coupling coefficients are represented by Q_e , K_{12} and K_{23} , respectively. Q_e can then be obtained by the following equation [23]:

$$Q_e = \frac{f_0}{\Delta f_{\pm 90^\circ}} \quad (3)$$

where f_0 denotes the resonance frequency of the first resonator (i.e., EMSIW resonator with number 1 or 4) near the excitation port, and $\Delta f_{\pm 90^\circ}$ is determined from the frequency at which the phase $\pm 90^\circ$ with respect to the absolute phase at f_0 .

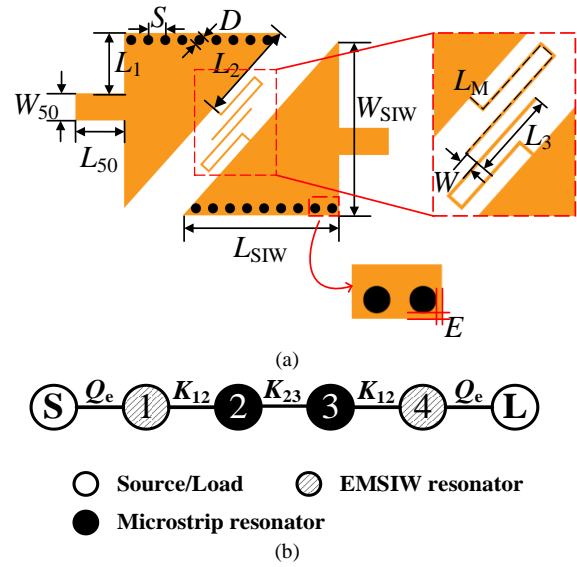


Fig. 1. (a) Layout and (b) the coupling topology of BPF I.

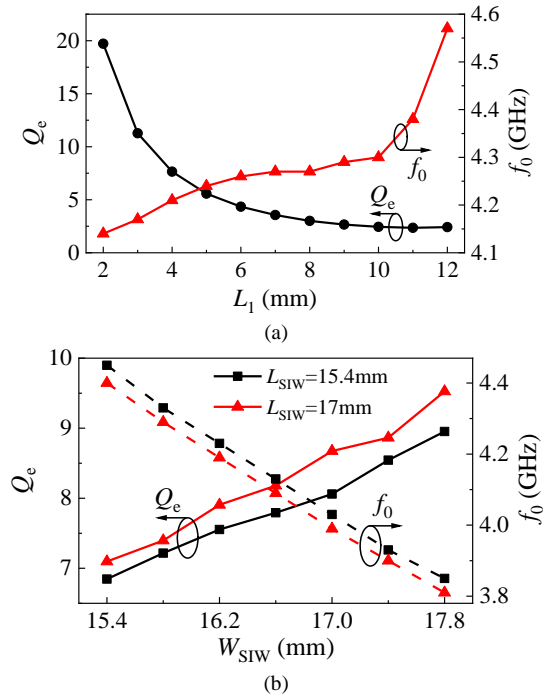


Fig. 2. Extracted results of Q_e and f_0 , (a) versus L_1 with $L_{SIW} = 16.2$ mm and $W_{SIW} = 16.2$ mm, (b) versus L_{SIW} and W_{SIW} with $L_1 = 4$ mm. ($W_{50} = 2.7$ mm, $L_{50} = 5$ mm, $S = 1.6$ mm, $D = 1$ mm)

The extracted Q_e and resonant frequency f_0 of EMSIW resonator are illustrated in Fig. 2. As shown in Fig. 2(a), when W_{SIW} and L_{SIW} are fixed, Q_e will decline with a large value of L_1 , which means that the proper value of the external quality factor could be obtained by choosing L_1 accordingly from the Q_e versus L_1 curve. However, the tendency of f_0 moving away from 4 GHz with the increase of L_1 will cause the final frequency response to be far away from expectation. To overcome such a problem, the size of EMSIW resonator will need adjustments. Fig. 2(b) presents the ability of W_{SIW} and L_{SIW} to control Q_e and f_0 . Increasing W_{SIW} will make Q_e higher and f_0 lower, while L_{SIW} is the opposite. Therefore, L_1 , W_{SIW} and L_{SIW} should be taken into consideration to achieve the suitable value of Q_e and keep f_0 around 4 GHz simultaneously.

TABLE I
DIMENSIONS OF THE BPF I

Para.	L_{SIW}	W_{SIW}	W_{50}	L_{50}	L_M	L_1
Value(mm)	15.4	17.6	2.7	5	14.5	6
Para.	L_2	L_3	W	S	D	E
Value(mm)	11(10.7*)	5	0.65	1.6	1	0.2

*The value in bracket stands for the initial dimensions.

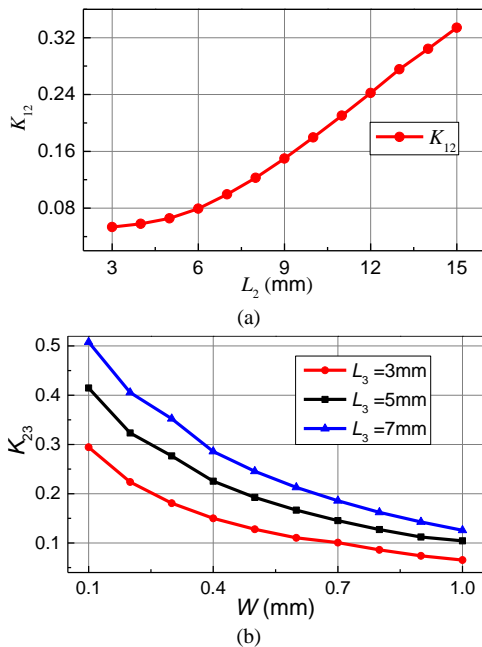


Fig. 3. (a) Extracted coupling coefficient K_{12} versus L_2 , and (b) extracted coupling coefficient K_{23} versus L_3 and W .

According to the calculated value of q_e in (2a), the dimensions of EMSIW (L_{SIW} and W_{SIW}) and position of feedline (L_1) can be determined accordingly and shown in Table I. The length of microstrip resonator (L_M) could be tuned to ensure its center frequency at around 4 GHz. Subsequently, the coupling coefficients can be extracted through the eigenmode simulation of the two coupled resonators [23]. The curves of K_{12} and K_{23} shown in Fig. 3 present a relationship between extracted results and physical dimensions. As illustrated in Fig. 3(a), K_{12} can be adjusted by changing the location of microstrip resonator on the hypotenuse side of EMSIW resonator (i.e., L_2). Fig. 3(b) shows that K_{23} is related to the length (L_3) and width (W) of the

coupling section between two microstrip resonators. Similarly, the values of L_2 , L_3 and W can be found immediately according to the calculated k_{12} and k_{23} . All of the rest dimensions are listed in Table I. Considering the influence of some parasitic effects, the designed BPF is slightly tuned and the final parameters are also shown in Table I. Through the eigenmode simulations, the unloaded quality factors (Q_u) of EMSIW resonator and microstrip resonator can be obtained, which are 496.9 and 216.5, respectively.

For demonstration, the fabricated BPF I is presented in Fig. 4(a). As shown in Fig. 4(b) and 4(c), the simulated and measured S-parameters and group delay agree well with each other. The measured insertion loss (IL) within the passband is 0.9 dB, while the return loss is better than 14.1 dB. The measured FBW is about 25.5% with center frequency at 4 GHz. The stopband rejection levels at the lower and upper sides of the passband are better than 20 dB from dc to 3 GHz ($0.75f_0$) and from 5.17 GHz ($1.29f_0$) to 9.56 GHz ($2.39f_0$), respectively. The spurious response is produced above 10 GHz. The size of BPF I excluding feedlines is 20.1 mm \times 19.6 mm ($0.268\lambda_0 \times 0.261\lambda_0$), where λ_0 denotes the guided wavelength at 4 GHz in free space.

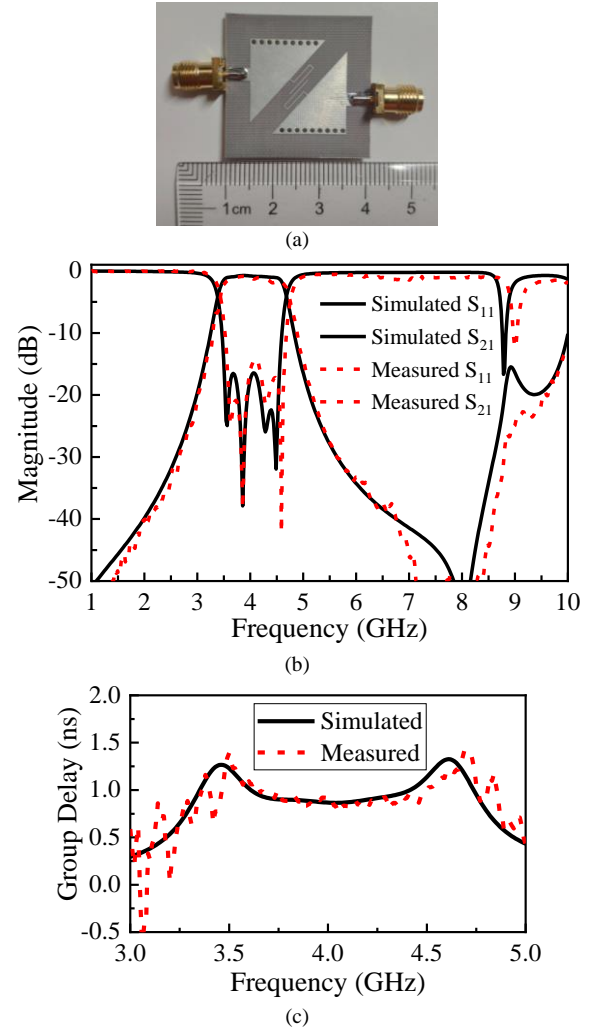


Fig. 4. (a) The photograph of the fabricated BPF I, and its simulated and measured (b) S-parameters and (c) group delay.

III. BPF II WITH MIXED ELECTRIC AND MAGNETIC COUPLING

In the topology of BPF I, two microstrip resonators incorporated in the EMSIW resonators are coupled with each other by the end of $\lambda/4$ lines, which means that only electric coupling contributes to the coupling scheme. Therefore, there is no TZ generated with such coupling topology of BPF I. To improve the performance out of passband, BPF II with a TZ is proposed by changing the configuration of microstrip resonators, which is shown in Fig. 5(a).

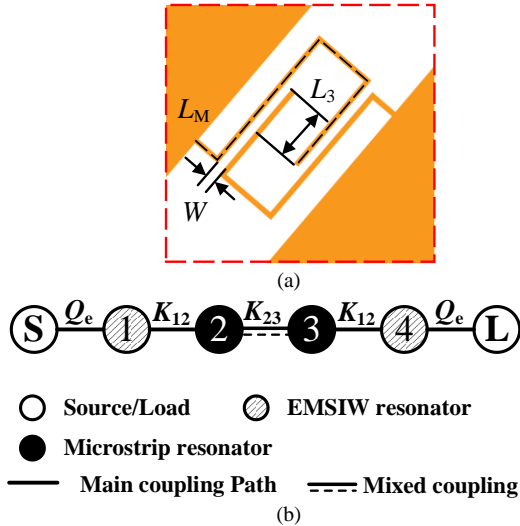


Fig. 5. (a) Partial layout and (b) the coupling topology of the BPF II.

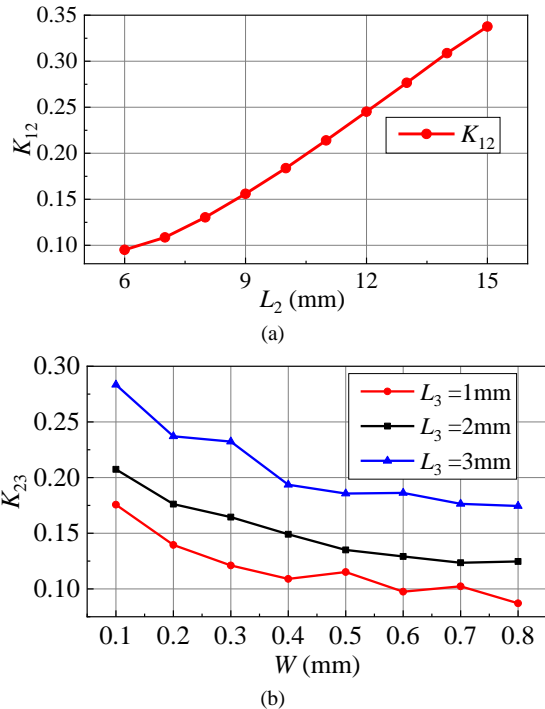


Fig. 6. (a) Extracted coupling coefficient K_{12} versus L_2 , and (b) extracted coupling coefficient K_{23} versus L_3 and W of the BPF II.

By creating the mixed electric and magnetic coupling in two coupled microstrip resonators, a TZ can be introduced without cross-coupling [24]. Fig. 5(b) shows the coupling scheme with mixed-coupling introduced. Following the same process, the coupling coefficients are extracted by eigenmode simulation and shown in Fig. 6. Total coupling coefficient K_{23} versus

different values of L_3 and W is used to determine the initial dimensions of proposed BPF. Due to the similar coupling topology with the BPF I, the coupling matrix \mathbf{M} synthesized in Section II could be utilized in the design process of BPF II. Without changing the specifications of BPF, the dimensions of BPF II are obtained according to the calculated q_e , k_{12} and k_{13} in Section II. In Table II, the dimensions of EMSIW are adjusted slightly to compensate for the parasitic effect.

TABLE II
DIMENSIONS OF THE BPF I

Para.	L_{SIW}	W_{SIW}	W_{50}	L_{50}	L_M	L_1
Value(mm)	15.3(15.4*)	17.9(17.6*)	2.7	5	13	6
Para.	L_2	L_3	W	S	D	E
Value(mm)	10.6	2	0.3	1.6	1	0.2

*The values in bracket stand for the initial dimensions.

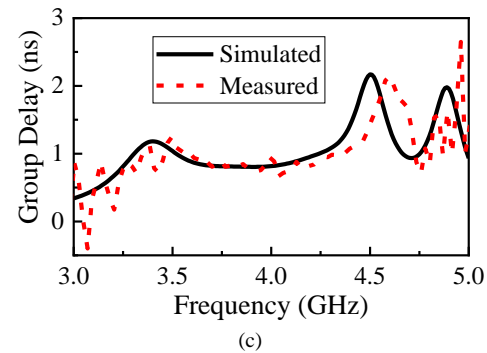
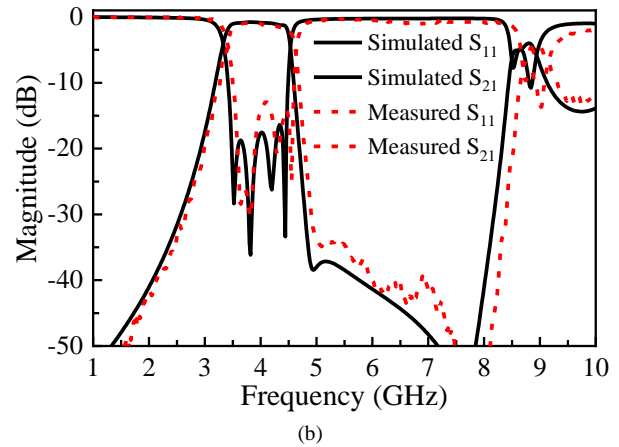
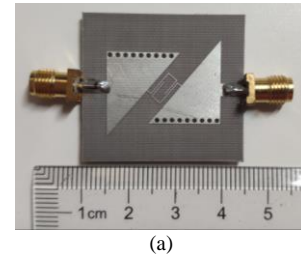


Fig. 7. (a) The photograph of the fabricated BPF II, and its simulated and measured (b) S-parameters and (c) group delay.

The BPF II is also fabricated on the substrate with the relative dielectric constant of $\epsilon_r = 2.65$ and thickness of $h = 1$ mm. The measured and simulated S-parameters along with group delay are shown in Fig. 7. There is good agreement between the simulated results and the measured results. The measured FBW of BPF II is 26.6% with the center frequency at 4 GHz. Moreover, the measured IL within the passband is about

0.8 dB, while the return loss is greater than 12.1 dB. The measured stopband rejection level at the lower side of passband is greater than 20 dB from dc to 2.98 GHz ($0.745f_0$), while the stopband rejection at the other side is better than 34 dB from 5.02 GHz ($1.26f_0$) to 8.31 GHz ($2.08f_0$). The harmonic response is yielded at about 8.84 GHz ($2.21f_0$). There is a TZ generated at the upper edge of the passband, which is located around 5.07 GHz, making sharper roll-off skirts and providing a better out-of-band rejection. Besides, the group delay of BPF II near upper edge of passband is higher than that of BPF I. Therefore, BPF II with higher group delay may contribute to designing the oscillator with better phase noise [19]. The size of BPF II excluding feedlines is 24 mm \times 20.7 mm ($0.32\lambda_0 \times 0.276\lambda_0$). For this case, the Q_u values of EMSIW resonator and microstrip resonator are 495.3 and 243.6, respectively. The performance comparisons between the proposed two BPFs and other reported works are tabulated in Table III.

TABLE III
PERFORMANCE COMPARISONS WITH SOME REPORTED BPFs

	f_0 (GHz)	Topology	FBW (%)	IL (dB)	Rejection level	Size ($\lambda_0 \times \lambda_0$)
[7] Work-3	8	QMSIW +EMSIW	11	1.3	>23 dB $1.1f_0$ - $1.96f_0$	0.483×0.304
[11]	3.7	HMSIW +CPW	6.7	1.49	>20dB up to $2.65f_0$	0.39×0.8
[16]	10	QMSIW +MR*	22.7	1.2	>36 dB $1.26f_0$ - $2f_0$	0.62×0.62
[17] Work-1	9.1	EMSIW +CPW	22	0.9	>10 dB $1.12f_0$ - $1.46f_0$	0.224×0.224
[18]	10.11	SIW + Microstrip	11.7	1.2	>20 dB up to $2.9f_0$	0.54×0.93
This work	BPF I	EMSIW +MR	25.5	0.9	>20 dB $1.29f_0$ - $2.39f_0$	0.268×0.261
	BPF II	EMSIW +MR	26.6	0.8	>34 dB $1.26f_0$ - $2.08f_0$	0.32×0.276

*MR means microstrip resonator.

IV. CONCLUSION

This paper proposes two compact BPFs with EMSIW resonators and microstrip resonators. Compared with traditional SIW resonators, EMSIW resonators is able to reduce the overall size and microstrip resonators can provide the flexibility for the filter design. Besides, a TZ is introduced with mixed electric and magnetic coupling between microstrip resonators while maintaining the same size. In the extraction process of Q_e , the dimensions of EMSIW cavity and the position of feedline are taken into consideration together to achieve the suitable value of Q_e and keep the resonance frequency unchanged simultaneously. It can reduce the difficulty of optimization after the initial dimensions are determined. Due to the simple structure and ease of design, the proposed BPFs are attractive for modern wireless communication technology.

REFERENCES

[1] T. R. Jones and M. Daneshmand, "Miniaturized folded ridged quarter-mode substrate integrated waveguide RF MEMS tunable bandpass filter," *IEEE Access*, vol. 8, pp. 115837-115847, 2020.
 [2] B. Chen, S. K. Thapa, A. Barakat and R. K. Pokharel, "A W-band compact substrate integrated waveguide bandpass filter with defected ground structure in CMOS technology," *IEEE Trans. Circuits Syst. II: Exp. Briefs*, vol. 69, no. 3, pp. 889-893, Mar. 2022.

[3] A. Iqbal, J. J. Tiang, C. K. Lee, N. K. Mallat and S. W. Wong, "Dual-band half mode substrate integrated waveguide filter with independently tunable bands," *IEEE Trans. Circuits Syst. II: Exp. Briefs*, vol. 67, no. 2, pp. 285-289, Feb. 2020.
 [4] A. Iqbal, J. J. Tiang, S. K. Wong, S. W. Wong and N. K. Mallat, "QMSIW-Based Single and Triple Band Bandpass Filters," *IEEE Trans. Circuits Syst. II: Exp. Briefs*, vol. 68, no. 7, pp. 2443-2447, Jul. 2021.
 [5] L. Li, Z. Wu, K. Yang, X. Lai and Z. Lei, "A novel miniature single-layer eighth-mode SIW filter with improved out-of-band rejection," *IEEE Microw. Wireless Compon. Lett.*, vol. 28, no. 5, pp. 407-409, May 2018.
 [6] P. Li, H. Chu and R. S. Chen, "Design of compact bandpass filters using quarter-mode and eighth-mode siw cavities," *IEEE Trans. Compon., Packag., Manuf. Techn.*, vol. 7, no. 6, pp. 956-963, Jun. 2017.
 [7] P. Kim and Y. Jeong, "Compact and wide stopband substrate integrated waveguide bandpass filter using mixed quarter- and one-eighth modes cavities," *IEEE Microw. Wireless Compon. Lett.*, vol. 30, no. 1, pp. 16-19, Jan. 2020.
 [8] X. J. Zhang, C. Y. Ma and F. Wang, "Design of Compact Dual-passband LTCC Filter Exploiting Stacked QMSIW and EMSIW," *Electron. Lett.*, vol. 51, no. 12, pp. 912-913, Jun. 2015.
 [9] S. K. Thapa, B. Chen, A. Barakat, K. Yoshitomi and R. K. Pokharel, "X-band feedback type miniaturized oscillator design with low phase noise based on eighth mode SIW bandpass filter," *IEEE Microw. Wireless Compon. Lett.*, vol. 31, no. 5, pp. 485-488, May 2021.
 [10] P. Chu, W. Hong, and L. L. Dai, et al., "A Planar Bandpass Filter Implemented With a Hybrid Structure of Substrate Integrated Waveguide and Coplanar Waveguide," *IEEE Trans. Microw. Theory Techn.*, vol. 62, no. 2, pp. 266-274, Feb. 2014.
 [11] W. Shen, "Extended-Doublet Half-Mode Substrate Integrated Waveguide Bandpass Filter With Wide Stopband," *IEEE Microw. Wireless Compon. Lett.*, vol. 28, no. 4, pp. 305-307, Apr. 2018.
 [12] K.-D. Xu, Y. Guo, Q. Yang, Y. Zhang, X. Deng, A. Zhang, and Q. Chen, "On-chip GaAs-based spoof surface plasmon polaritons at millimeter-wave regime," *IEEE Photon. Technol. Lett.*, vol. 33, no. 5, pp. 255-258, 2021.
 [13] Z. He, C. J. You, S. Leng, X. Li and Y. -M. Huang, "Compact bandpass filter with high selectivity using quarter-mode substrate integrated waveguide and coplanar waveguide," *IEEE Microw. Wireless Compon. Lett.*, vol. 27, no. 9, pp. 809-811, Sept. 2017.
 [14] G. Lin and Y. Dong, "A Compact, Hybrid SIW Filter With Controllable Transmission Zeros and High Selectivity," *IEEE Trans. Circuits Syst. II: Exp. Briefs*, vol. 69, no. 4, pp. 2051-2055, Apr. 2022.
 [15] A. Iqbal, J. J. Tiang, S. K. Wong, M. Alibakhshikenari, F. Falcone, and E. Limiti, "Multimode HMSIW-based bandpass filter with improved selectivity for fifth-generation (5G) RF front-ends," *Sensors*, vol. 20, no. 24, p. 7320, 2020.
 [16] Y. Zheng, Y. Zhu, Z. Wang and Y. Dong, "Compact, wide stopband, shielded hybrid filter based on quarter-mode substrate integrated waveguide and microstrip line resonators," *IEEE Microw. Wireless Compon. Lett.*, vol. 31, no. 3, pp. 245-248, Mar. 2021.
 [17] X. Wang, X. W. Zhu, and Z. H. Jiang, et al., "Analysis of eighth-mode substrate-integrated waveguide cavity and flexible filter design," *IEEE Trans. Microw. Theory Techn.*, vol. 67, no. 7, pp. 2701-2712, Jul. 2019.
 [18] Y. Zhu and Y. Dong, "A Novel Compact Wide-Stopband Filter With Hybrid Structure by Combining SIW and Microstrip Technologies," *IEEE Microw. Wireless Compon. Lett.*, vol. 31, no. 7, pp. 841-844, Jul. 2021.
 [19] X. Wang, Z.-Y. Zong, and W. Wu, "Low phase noise oscillator employing miniaturized shielded-EMSIW resonators embedded with CSRRs structure," *AEU-Int. J. Electron. Commun.*, vol. 151, Jul. 2022.
 [20] S. Sirci, M. A. Sanchez-Soriano and J. D. Martinez, et al., "Design and Multiphysics Analysis of Direct and Cross-Coupled SIW Combine Filters Using Electric and Magnetic Couplings," *IEEE Trans. Microw. Theory Techn.*, vol. 63, no. 12, pp. 4341-4354, Dec. 2015.
 [21] Y. Cui, K.-D. Xu, Y. Guo, and Q. Chen, "Half-mode substrate integrated plasmonic waveguide for filter and diplexer designs," *J. Phys. D: Appl. Phys.*, vol. 55, p. 125104, 2022.
 [22] R. J. Cameron, C. M. Kudsia, R. R. Mansour, *Microwave Filters for Communication Systems: Fundamentals, Design and Applications*, 2nd ed., New York (USA): John Wiley and Sons, 2018.
 [23] J.-S. Hong, M. J. Lancaster, *Microstrip Filters for RF/Microwave Applications*, 2nd ed., New York (USA): John Wiley and Sons, 2005.
 [24] Q. Chu and H. Wang, "A compact open-loop filter with mixed electric and magnetic coupling," *IEEE Trans. Microw. Theory Techn.*, vol. 56, no. 2, pp. 431-439, Feb. 2008.